FTIR Remote Sensing of Biomass Burning Emissions of CO_2, CO, CH_4, CH_2O, NO, NO_2, NH_3, and N_2O

David W. T. Griffith, William G. Mankin, Michael T. Coffey, Darold E. Ward, and Allen Riebau

Global biomass burning plays an important role in the budgets of many species in atmospheric chemistry. Recent estimates suggest that 3 to 6 Petagrams (1 Pg = 10^{15} g) of carbon are burned globally as biomass each year (Crutzen and Andreae, 1990; Seiler and Crutzen, 1980), an amount similar in magnitude to that burned as fossil fuel. In contrast, however, biomass burning takes place less efficiently, and both fuel and fire characteristics vary widely, resulting in the emission of a far more complex mixture of species to the atmosphere. To understand the role of biomass burning in atmospheric chemistry, it is essential not only to identify and quantify these emissions but also to understand their dependence on the fuel and fire characteristics which determine them. These characteristics include such parameters as fuel composition and moisture content, fuel loadings and fire intensity, meteorology, and type of combustion (e.g., flaming, smoldering, or glowing). Only with such an improved understanding will we be able to make reliable assessments of future emissions and feedbacks from biomass burning in a world of changing climate.

A growing number of studies have made significant progress in characterising biomass burning emissions (e.g., Crutzen et al., 1979, 1985; Greenberg et al., 1984; Delany et al., 1985; Andreae et al., 1988; Cofer et al., 1989, 1990; Lobert, 1989; Hegg et al., 1990), resulting in a growing collection of data. The results are normally quoted as relative emission ratios, defined as the amount (in moles) of substance emitted divided by that of CO_2, CO, or of fuel burned; these emission ratios can then be multiplied by estimates of regional or global emissions of CO_2 or CO or fuel burned to arrive at regional or global estimates of biomass burning emissions. Natural variability in meteorology, biomass, and fire types causes these measured emission ratios to vary widely, by factors of 4 to 5 or more, and the detailed relationships between the emissions and their determining parameters remain unclear. In addition, different techniques may introduce systematic differences, especially where reactive or difficult-to-measure species (such as NO_x and NH_3) are involved. All measurements to date have been made by conventional methods for atmospheric trace gas analysis, using either in situ instruments or grab sampling with subsequent laboratory analysis. In general, one technique can be used for the analysis of one species (or class of species); to obtain an overview of smoke plume composition, coordinated measurements from several techniques are required. This overview is, however, essential to the understanding of the many relationships between emissions and the controlling fire characteristics.

This work introduces remote sensing of biomass burning emissions using high-resolution Fourier transform infrared (FTIR) absorption spectroscopy over open paths in smoke plumes from biomass fires. There are several advantages to this type of smoke composition measurement, which address some of the disadvantages of previous measurements:

- Simultaneous measurements of a wide range of gas phase species in the smoke can be made with a single technique.
- Pseudo-continuous measurements may be made before, during, and after a fire.
- The technique is a remote sensing technique; no sampling is required, so there are no uncertainties due to loss or production of species in sample transfer lines or containers.
- Measurements are integrated over a long path through the smoke plume and therefore are not subject to small-scale local variations as may be the case with in situ and grab-sampling methods.

This technique provides an overview of the combustion products from burning not available from any other single technique used to date and can yield much valuable information on the gaseous emission products from biomass burning and the factors which control the balance of those emissions.

Using FTIR absorption spectroscopy over long, open paths, we have made measurements of the smoke composition from sagebrush and forestry slash

Levine, J.S. (ed), 1991. Global Biomass Burning: Atmospheric, Climatic, and Biospheric Implications. Cambridge, MA: MIT Press.

fires in rural areas of Wyoming and Montana, and from various fuels in the stack of a large-scale combustion laboratory. In this chapter we report a preliminary analysis of the spectra obtained from the field studies and present simultaneous measurements of CO_2, CO, CH_4, CH_2O, NO, NO_2, NH_3, N_2O, and HCN in the plumes of four fires.

Experiment Procedure

In summary, the experiment consists of a Fourier transform spectrometer with suitable input optics collecting infrared radiation from a collimated IR source up to 200 meters (m) distant in field measurements, and 3 m distant in the laboratory stack. Smoke from field or laboratory fires passes through the infrared beam between source and spectrometer, and IR spectra of the smoke are recorded continually before, during, and after a fire. Subsequent analysis of the IR absorption spectra yields simultaneous concentrations of many gas-phase species, averaged over the optical path.

FTIR Spectrometer

The Fourier transform spectrometer consisted of a Michelson interferometer (EOCOM Corp.) with a Ge/KBr beamsplitter, a range of selectable optical filters, an InSb/MCT sandwich detector, and a controlling PDP-11/23 minicomputer (Mankin, 1978). Interferograms were written directly as collected onto one-half–inch magnetic tape for later processing. The interferometer had a maximum resolution of 0.06 cm^{-1} (apodized), but was used at 0.12 cm^{-1} in all measurements because absorption lines typically have widths of 0.15 cm^{-1} due to atmospheric pressure-broadening. Spectra were recorded alternately in the regions from 700 to 1900 cm^{-1} (MCT detector, no optical filter) and 1800 to 3900 cm^{-1} (InSb detector, 2.5μm short wavelength cutoff filter). A single scan required 5 to 10 seconds; spectra were collected and coadded in groups of 5, 10, 20, or 40 scans depending on the signal level and time resolution required. Time resolution for coadded scans was thus 0.5 to 4 minutes.

Field Measurements

The optical arrangement for long-path field studies is illustrated in Figure 30.1. The input optics for the interferometer consisted of a 300 millimeter (mm) diameter periscope (M1 & M2) to allow for beam height adjustment and pointing at the source, a 300

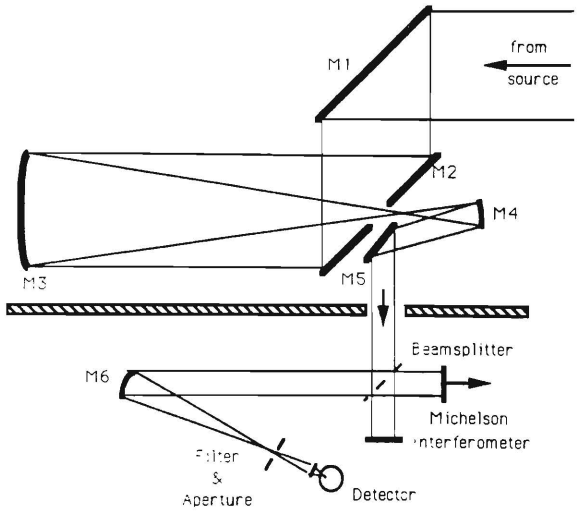

Figure 30.1 Schematic diagram of the FTIR long-path absorption spectrometer in field use.

mm diameter × 1 m focal length (f.l.) spherical mirror (M3) to focus and collect the incoming beam, and a 50 mm diameter × 200 mm f.l. spherical mirror (M4) to recollimate the collected beam into the interferometer.

The spectrometer assembly, computer, and tape drive were mounted in a 2 × 3 m enclosed trailer, with entry for the IR beam through rear double doors. Power was supplied by a 2.2 k VA Honda petrol generator. The source, located 25 to 200 m distant dependent on fire site and local topography, was a silicon carbide gas furnace igniter (Carborundum Corp., 28 V, ca. 150 Watt) powered by a small (400 VA) generator. The source was collimated by a 250 mm diameter Cassegrain telescope mounted on a tripod. When the source is focused by its telescope onto the input aperture of the receiver telescope, and the receiver telescope focuses the source telescope onto the input aperture of the interferometer, the throughput of the entire optical system is interferometer-limited at source-receiver separations less than about 140 m; at greater pathlengths light is effectively lost due to the lower throughput of the long path, and signal-to-noise ratios are degraded. In practice, under field conditions, although the two telescopes could be accurately and stably aligned with one another, the focussing was less precise, and some signal was lost. Signal was also lost through distortion of the beam by the two aluminised plate glass periscope mirrors, which were not optically flat.

In operation, a site was chosen over or upwind of the proposed fire site, and the trailer and source set

up. Visual alignment of source and receiver telescopes was usually sufficient to obtain a signal through the interferometer, which could then be maximized by fine adjustment of the first periscope mirror and source telescope. The telescope alignment was then stable for several hours, although temperature changes of up to 15°C occurred through the day, necessitating some interferometer realignment. The trailer and source could usually be set up in one to two hours by two people. Spectra were recorded before ignition to determine background atmospheric composition, then continuously for the duration of the fire.

Laboratory Measurements

The laboratory experiments were carried out in the large-scale combustion laboratory of the Intermountain Fire Sciences Laboratory, U.S. Forest Service, Missoula, Montana. The combustion laboratory consists of a large room (about 12 × 12 × 20 m L × W × H) with controllable temperature and humidity, a large "inverted funnel" with a 1.5 m diameter exhaust stack above the fuel bed, and an observation platform with sampling ports and windows in the stack 15 m above the fuel bed. The spectrometer and source were installed on the platform for measurement of cross-stack spectra. The IR source (the same as for field experiments) was collimated by a 75 mm diameter spherical mirror, traversed the stack twice (for a total smoke path length of 3 m), and was directed by a flat mirror into the interferometer. Signal levels were typically five times higher than in field experiments, resulting in spectra with good signal to noise ratios (>200:1) from 5 to 10 scans in 30 to 60 sec. Spectra were recorded before ignition and continuously until burnout. A typical burn time for 30 kg fuel was 1 hour.

In parallel to the IR measurements, stack temperature and flow and fuel bed weight were continuously measured, and samples were withdrawn continuously and monitored for CO_2, CO, NO, and NO_x using NDIR and chemiluminescence instruments. Filter samples for particulates were also collected.

More details of the laboratory measurements will be published separately; in this chapter, only preliminary results relevant to field measurements will be presented.

Description of Fires

Measurements were made during five prescribed burns of sagebrush scrub land (Wyoming) and coniferous forest waste (Montana). The individual fires are next described in detail.

• *F1:* 3 October 1989, Muddy Springs, 50 km south of Casper, Wyoming, on open high plains, elevation 2200 m. Vegetation burned was sagebrush scrub interspersed with thin grass. Weather was dry, sunny, and cool, with a light southerly wind following a cool change. Air temperature was below 0°C overnight, warming to 13°C and relative humidity 49% at noon. The spectrometer and source were located 107 m apart across a shallow (4 to 5 m) valley. The valley was burned from below; the fire front moved up-valley, through the IR beam to the top of the gully. Spectra were recorded from before the first arrival of smoke from below, through the flaming of sagebrush directly under the beam, and continued well through final smoldering. Ignition of sagebrush was fast, with flame heights reaching 2 to 3 m, and almost total combustion of above-ground biomass.

• *F2:* 5 October 1989, Curry Creek, 20 km south of F1 at Muddy Springs. Vegetation was as for Muddy Springs, but on a flat site. Temperature and relative humidity were 2°C and 69% respectively at 9:30, warming to 6 to 8°C during the burn. Wind was light northerly. The path was 170 m long and 2 m above ground over the flat terrain on the downwind edge of a 200 × 200 m plot which was burned starting from the upwind edge. Background spectra were recorded for 30 minutes before ignition, and continuously in smoke for 1.5 hours after ignition. During this fire, detailed measurements of meteorological and fire parameters and plume characteristics were also made (A. Riebau and M. Sestak, to be published).

• *F3:* 16 October 1989, Ward Canyon, Lolo State Forest, 100 km west of Missoula, Montana. Fires were of piled waste from forestry operations in mixed pine/fir/larch forest in hilly terrain. Slash piles were mainly made up of stemwood and branches 30 to 40 cm in diameter, typically 4 × 4 m × 2 to 3 m high, with little fine fuel, needles, or litter. The piles burned initially with good flaming combustion and little visible smoke. The 128 m optical path was set up parallel to and immediately upslope (downwind) of a line of three piles which were ignited together at 13:00. Weather was clear and dry, temperature 6 to 8°C. Spectra were recorded before and for three hours during the burning of the slash piles. Early spectra in the sequence, when flaming was intense, were complicated by emitted radiation from the hot flames and plumes.

• *F4:* 17 October 1989, site and conditions as for F3. Spectra were recorded directly of the IR emission from flames, plume, and coals of a slash pile fire similar to that described for F3. Due to the high

temperatures of the IR-emitting plume gases, the spectra are more complicated than the simple absorption spectra. Analysis of these spectra will be reported separately.

• *F5:* 18 October 1989. Gold Creek, Lolo National Forest, 30 km northeast of Missoula, Montana. Weather was clear and dry. This fire was again a burn of waste from logging operations in pine/larch forest and in this case, a broadcast burn, in which the waste branches, small fuel, and some logs were left scattered on the ground, and the fire propagated across the ground through the site. The site was about 2 hectares of sloping hillside, ignited along the top edge, so that the fire spread slowly downhill, burning the whole site in about six hours. The spectrometer and source were set up across the uphill edge of the site, with a path length of 32 m which was totally immersed in the smoke from the fire below. No spectra were recorded of the background before ignition due to an instrument fault; spectra of smoke were recorded for two hours, beginning about two hours after initial ignition.

Analysis of Spectra

There are several possible approaches to the quantitative analysis of IR absorption spectra, ranging from the simple comparison of measured peak heights or areas with those from calibration spectra, to a more precise least-squares fitting of observed to calculated spectra. The preliminary analyses presented here were made by comparison of peak height or area measurements with calibration spectra. The "calibration" spectra are in this case *calculated* spectra for a wide range of compositions of the various absorbing species. The spectral calculation program for generating "calibration" spectra assumes a homogeneous path through mixtures of a given composition, pressure, and temperature. Absorption line parameters (positions, strengths, line widths, and temperature dependencies) were taken from the AFGL atmospheric line parameters compilation (Rothman et al., 1983, 1987). The calculated spectra include the effects of pressure and Doppler broadening (i.e., the Voigt profile) and apodization.

For each molecule of interest, absorption lines which were reasonably clear of other features in the spectrum were selected to minimize interferences and local baseline variations. The lines were also chosen to have absorptions of less than about 70% to avoid excessive nonlinearities. Spectra in each region containing selected absorption lines were then calculated for a range of concentrations of the molecule of interest and included other absorbers in that spectral region. Peak heights and areas for the selected absorption lines were then measured from a local baseline, and a calibration curve of absorption vs concentration was generated for each line. From the calibration for each line used, the path-averaged concentration of absorber was retrieved from the corresponding peak heights in the experimental smoke plume spectra. Reported concentrations are the means of the retrievals from all lines used for each molecule. The absorption lines used in the analyses are tabulated in Table 30.1, and Figures 30.2 and 30.3 show two examples of measured and calculated spectra in the regions containing CO, CO_2, and NH_3 absorption.

The systematic errors associated with these calibrations primarily reflect the accuracy of the AFGL line parameters, typically 5% to 10% (Rothman et al., 1983, 1987). Other sources of systematic error should be small by comparison; these include the lineshape calculation in calibration spectra, pressure and temperature variations, and any systematic differences between the measured and calculated spectra due to instrumental distortions and nonlinearities, phase errors, etc. Random error is due principally to noise in the spectra, and the consequent errors in measuring local baseline and peak absorption. These errors vary

Table 30.1 Absorption lines used in quantitative analysis of spectra

Molecule	Lines (cm^{-1})	Detector	Precision (%)
CO_2	2047.5, 2056.7, 2062.8	InSb	10
CO_2	723.9, 725.5, 727.0, 733.2, 734.7, 736.2, 737.8, 739.3, 746.8, 749.8	MCT	25
CO	2050.8, 2055.4	InSb	5
CH_4	2917.6, 2926.8, 2938.2, 2948.4, 3038.5	InSb	7
CH_2O	2778.5, 2781.0	InSb	20
N_2O	2201.7, 2207.6, 2211.4, 2214.2, 2216.8	InSb	4
NO	1900.1, 1903.1, 1906.0	InSb	45
NO_2	1598.4, 1598.9, 1599.9	MCT	70
NH_3	867.9, 892.2, 951.8, 967.3, 992.7, 1007.5, 1027.0, 1046.4, 1103.4, 1140.6	MCT	15

Note: Alternate spectra were recorded using MCT and InSb detectors. The precision values are estimates of the relative errors in retrieved mixing ratios, determined from the observed noise levels in each region, and the variance in each set of determined mixing ratios for each species.

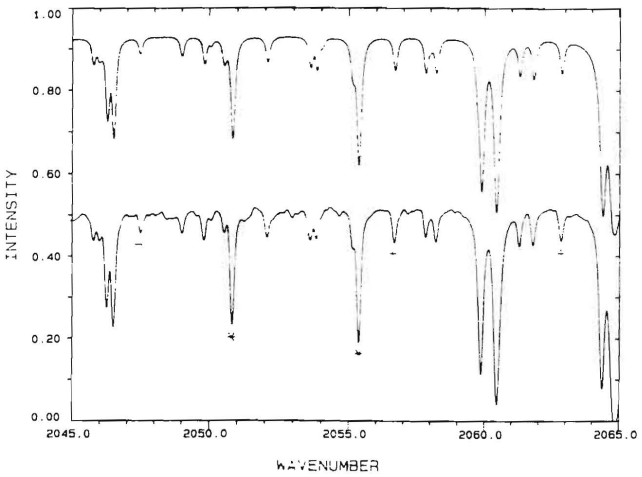

Figure 30.2 Typical spectra from 2045 to 2065 cm^{-1} showing lines used for CO_2 (+) and CO (*) analyses. Lower trace: measured spectrum beginning at 12:46 from fire F2 (InSb detector, 40 scans). Upper trace: calculated spectrum (path 177 m; temperature 7°C; pressure 0.8 atm; H_2O 4500 ppm; CO_2 690 ppm; CO 35 ppm).

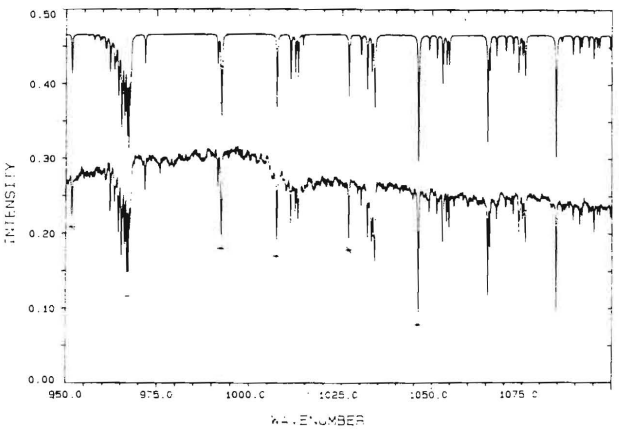

Figure 30.3 Typical spectra in the 1000 cm^{-1} region used for NH_3 analyses. Lower trace: measured spectrum beginning at 12:43 from fire F2 (MCT detector, 80 scans). Upper trace: calculated spectrum (path 177 m; temperature 7°C; pressure 0.8 atm; H_2O 4500 ppm; NH_3 1.3 ppm). NH_3 lines used in the analyses are marked with an asterisk (*).

from molecule to molecule and in different regions of the spectrum. Estimated percent errors are included in Table 30.1, and are based on both the observed signal-to-noise ratio and the measured line-to-line variation in retrieved concentrations for each molecule.

This method of analysis measures the total column amount of an absorber in the optical path. For all later discussion, these absorber column amounts are converted to path-averaged mixing ratios using the measured optical path length, atmospheric pressure, and temperature. Since the results are ultimately quoted as emission ratios relative to CO_2, any systematic error in calculating the path-averaged mixing ratios will cancel out. The actual mixing ratios in the plumes usually exceed the path-averaged values, since normally only a part of the optical path actually contains smoke at any one time.

Results

In all, 115 absorption spectra of the four prescribed burns were recorded. We present here detailed concentration and emission ratio chronologies of several species for fire F2, and averages for all four fires.

Analysis of the spectra as described above yields initially path-averaged mixing ratios for a number of species as a function of time with three- to five-minute resolution. Figure 30.4 shows the temporal changes of CO_2 and CO mixing ratios in the plume from the second sagebrush burn, F2. The coarse features of these time series can be interpreted in terms of visual observations of the fire behavior. The time marked A in the plot corresponds to the first arrival of smoke in the beam. This smoke originated from combustion about 200 m upwind. At time B, fuel directly under the beam began to burn near the source, and the spectra for the next 15 minutes correspond to smoke immediately above flames. At time C, more fuel immediately beneath the beam was ignited, after which the fire subsided to smoldering combustion.

Emission ratios relative to CO_2 are of more interpretive value than raw mixing ratios and remove some systematic errors. The emission ratio for species X is calculated as

$$\text{Emission ratio } (X) = \frac{\text{Excess } X \text{ over background (ppm)}}{\text{Excess } CO_2 \text{ over background (ppm)}}$$

and stated as mole fraction, mole percent, or parts per thousand (per mil, or mmol/mol). Figure 30.5 shows

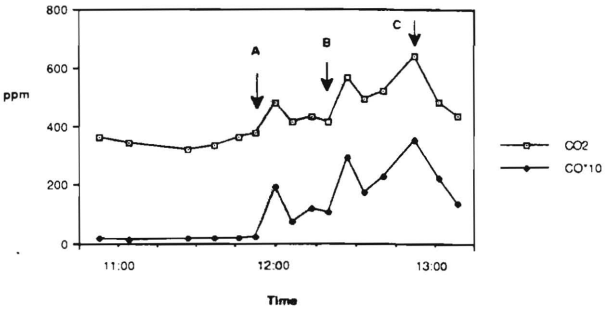

Figure 30.4 Path averaged mixing ratios of CO_2 and CO from sagebrush fire F2 as a function of time. The CO values have been multiplied by 10 for clarity. Times A, B, and C are discussed in the text.

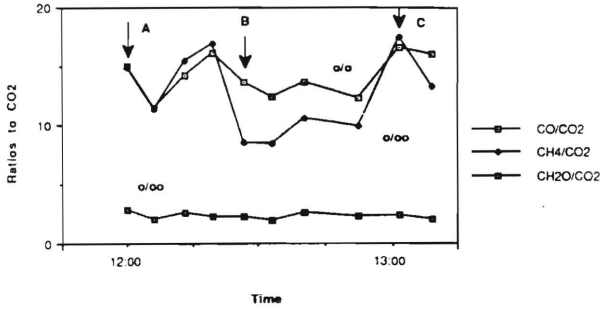

Figure 30.5 Emission ratios of carbon species CO, CH_4, and CH_2O relative to CO_2 as a function of time. For CO the units are mole percent, for CH_4 and CH_2O they are mmol/mol.

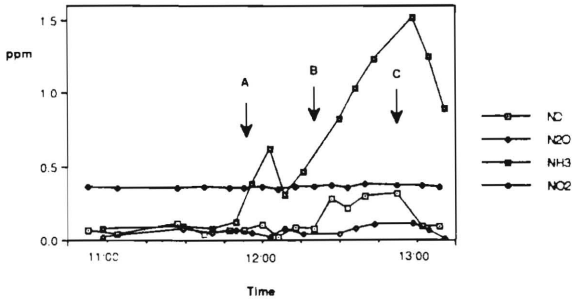

Figure 30.6 Path averaged mixing ratios of NO, NO_2, NH_3, and N_2O as a function of time for sagebrush fire F2.

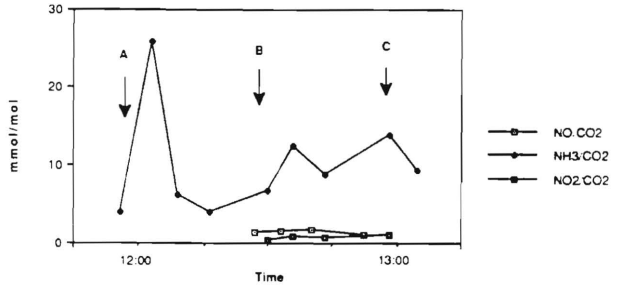

Figure 30.7 Emission ratios of nitrogen species NO, NO_2, and NH_3 relative to CO_2 as a function of time. All units are mmol/mol.

the emission ratios for CO, CH_4, and CH_2O as a function of time for fire F2. (Note change of timescale from Figure 30.4.) In this fire, the CO/CO_2 ratios vary from 12% to 16% with a mean of 14.1 ± 1.7% (one standard deviation), with lower values during flaming combustion, and higher values during smoldering. The CH_4 emission ratio varies by a factor of 2 between flaming and smoldering (8 to 17, mean 12.7 ± 0.3 mmol/mol), while CH_2O shows a fairly constant emission ratio of 2.3 ± 0.3 mmol/mol.

Figures 30.6 and 30.7 show similar data for the nitrogen-containing species NO, NO_2, NH_3, and N_2O. For most of the duration of the fire NO and NO_2 were at or below the detection limits of about 0.1 and 0.05 ppm, respectively, and were emitted in measurable concentrations only in relatively thick smoke. Nevertheless, it is clear that ammonia is the major IR-absorbing nitrogen compound in the smoke. NH_3 is on average about five times more abundant than NO_x (NO + NO_2), and NO appears to be dominant over NO_2. Neglecting the one apparently high value of NH_3/CO_2 (see below), the mean emission ratios for NH_3, NO, and NO_2 relative to CO_2 are of the order of 8, 1.4, and 0.8 mmol/mol, respectively. The precision of the data do not warrant further detailed analysis in terms of flaming/smoldering differences. In MCT spectra (NH_3 and NO_2) the precision in the determined emission ratios is mainly limited by the poor (25%) precision for the CO_2 measurements, which must be made from a weak band at the cutoff of the detector response. The high measured NH_3/CO_2 value at 12:03 is due to an apparently low CO_2 measurement from that spectrum. In addition, NO and NO_2, as pointed out above, are near detection limit and precision is also poor. In contrast to other techniques, however, the detection limit and precision for NH_3 are good.

The measurements of N_2O warrant special mention. As can be seen from Figure 30.6, there is no measurable change in the path-averaged N_2O mixing ratio before or during the fire. Given the precision for individual N_2O measurements of about 4% (and hence a precision for difference measurements from background of about 6%), we conclude that N_2O did not increase in the smoke at any time by more than 6%, or 20 parts per billion (ppb). For an excess CO_2 mixing ratio of 250 parts per million (ppm), this corre-

Table 30.2 Mean emission ratios relative to CO_2 for fires F1–F3, F5

Species	F1	F2	F3	F5
CO	181	141	183	196
CH_4	12.5	12.7	11.4	16.3
CH_2O	2.4	2.3	1.9	2.1
NO	0.8	1.1	<0.5	<1.5
NO_2	0.4	0.6	<0.4	<1.0
NH_3	8.4	8.3	1.4	3.3
HCN	0.3	0.1	<0.3	<0.2

Note: All values are in parts per thousand (mmol/mol), and are the average of all measurements above background for each fire.

sponds to an upper limit to the emission ratio relative to CO_2 of less than 8×10^{-5}.

Similar analyses were made for all fires, and the results are summarized as emission ratios relative to CO_2 in Table 30.2 and Figure 30.8. These data represent the averages of all measurements made above background for each fire. There are only minor differences between the relative average emissions of CO, CH_4, and CH_2O from the four fires, despite their being very different in nature. Figure 30.8b shows clearly that NH_3 is the major nitrogen-containing gas-phase species measured in all fires. Fires F1 and F2 had similar fuel and burning conditions and showed very similar emissions: a total N:C ratio of the order of 1%, with the NH_3:NO_x ratio of the order of 5:1. In F1 and F2, traces of HCN were also measured with concentrations of about 5% to 10% of NO_x. N_2O emission is insignificant by comparison to the other nitrogen species. Fires F3 and F4 showed significantly less nitrogen emission; in each case NO and NO_2 were below detection limits, and NH_3 was the only nitrogen-containing gas detected. This can be related to fuel nitrogen contents, which are discussed below.

Finally, we briefly report results from three laboratory fires which will bear on our later discussion. The fuel beds for these fires were chosen to consist of the same fuels as were burned in the field studies, and consisted of (1) sagebrush, (2) dead, dry pine needles, and (3) a mixture of needles, litter, and wood simulating the broadcast burn F5. In each case the flaming and smoldering combustion phases were well separated in time, and we have selected individual spectra recorded during each phase of each fire and analysed them for CO_2, CO, NO, NO_2, and NH_3. Figure 30.9 summarizes the results: for flaming and smoldering combustion in each fire, Figure 30.9a shows the emission ratios relative to CO_2 for CO and CH_4, and Figure 30.9b shows the emission ratios for NO, NO_2, and NH_3. The increase in CO and CH_4 emission ratios from totals of less than 3% during flaming to more than 12% during smoldering combustion is clear from Figure 30.9a. In Figure 30.9b, flaming emissions are dominated by NO and NO_2, while NH_3 is dominant during smoldering combustion. Both NO and NO_2 were below detection limits in the FTIR spectra in the smoldering phases of the pine-needle and broadcast-simulation fires. There is a suggestion that total detected nitrogen emissions are lower during the flaming phase, but in view of experimental error for these individual spectra this may not be significant.

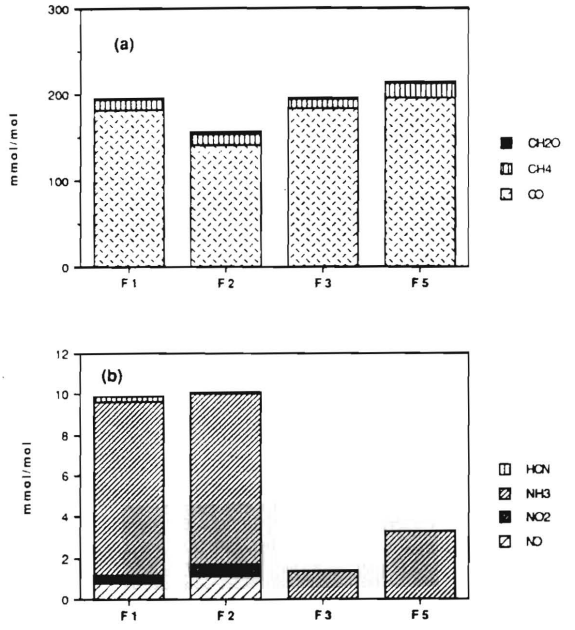

Figure 30.8 Mean emission ratios relative to CO_2 for all fires. (a) Carbon species. (b) Nitrogen species. All values are in mmol/mol, and are the average of all measurements above background for each fire.

Discussion

Technique

The study has demonstrated the utility of FTIR long-path spectroscopy for the measurement of many species in smoke from biomass burning. The principle advantages of the technique are its ability to measure many species simultaneously and pseudo-continuously in the same smoke sample, and the remote sensing advantage, i.e., that there are no uncertainties derived from the handling of smoke samples.

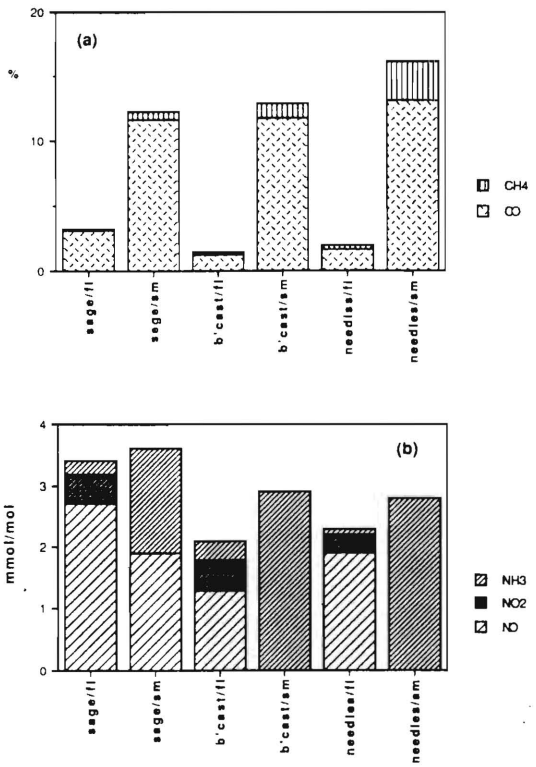

Figure 30.9 Emission ratios relative to CO_2 for (a) CO and CH_4 and (b) NO, NO_2, and NH_3 for three laboratory fires during the flaming and smoldering phases. Units are % for CO and CH_4, and mmol/mol for NO, NO_2, and NH_3. See text for details of fires.

Detection limits with the instrumentation used were of the order of 50 to 100 parts per billion (ppb) over a 100 m path for most molecules exhibiting infrared absorption spectra. The main species emitted by biomass burning which are not detected by FTIR are probably N_2 and H_2. The instrumentation could be set up in the field in one to two hours including all alignment procedures after transport to the site, could be realigned within a site in 20 to 60 minutes, and worked reliably under all field conditions encountered. In all, only one hour of data was lost due to instrument malfunction (and that turned out to be trivial!). The principle limitations are derived from the fact that the measurement is ground based and relatively immobile. It is therefore effectively restricted to prescribed burning measurements, where the fire site and approximate behavior, and wind conditions, are known in advance. Our measurements were restricted to smoke close to the ground and may therefore be biased against vigorous combustion which creates a buoyant, rapidly rising plume. The use of towers or steep terrain would mitigate this disadvantage.

There is considerable scope for improvement in both measurement precision and detection limits. Improvements are possible in both optical design and quantitative analysis of spectra. The long-path optical system used here was put together quickly using existing optical components that were not necessarily optimal for the task. The IR throughput of the entire system was about 20% of that without long-path optics, and with a more efficient design and better components, most of this loss of light should be regained, translating directly to a fivefold reduction in detection limits and a similar increase in precision. The major loss of throughput can be traced to the two large, flat mirrors used in the periscope for beam height adjustment and pointing. These mirrors were aluminized plate glass, and their lack of flatness over the large dimensions (300 × 420 mm) introduced distortion of the focussed beam. Optically flat mirrors of this dimension would be very expensive; a better solution would be to not use such mirrors at all and point the telescope directly. The second major source of throughput loss was the inability to easily focus the two telescopes under field conditions; this facility must be built into the mirror mounting designs. A further valuable improvement would be the use of two data channels in the FTIR spectrometer, permitting the recording of interferograms from both MCT and InSb detectors simultaneously instead of alternately. This would allow truly continuous measurements of all species at all times.

A second avenue for improvement lies in spectral analysis and quantitative retrieval of molecule concentrations from spectra. In the present analysis we have used the simplest option of comparing measured peak heights to those from calibration spectra. Better precision and detection limits should be possible using least-squares fitting procedures to match observed with calculated spectra. This improvement arises because many lines or a whole band are effectively used in the analysis for a given species instead of the few lines used here (Haaland and Eastman, 1980; Ying and Levine, 1989). The application of such fitting techniques to our existing spectra will be particularly useful in obtaining better excess CO_2 concentrations (which currently limit the precision of all measured emission ratios), lowering the detection limits for NO and NO_2, and giving a better measure of N_2O emissions. This analysis is underway.

Emissions from Biomass Burning

The fire-averaged results for emission ratios relative to CO_2 can be compared first to results of other

studies. CO measurements range from 5% to 25%, with values below 10% being typical from aircraft-based sampling (e.g., Andreae et al., 1988; Cofer et al., 1989, 1990; Hegg et al., 1990) and values above 10% from ground-based sampling (e.g., Crutzen et al., 1979, 1985; Greenberg et al., 1984). In addition, our laboratory measurements, and those of Lobert (1989; also Lobert et al., 1990) indicate that flaming combustion generally results in $CO:CO_2$ emission ratios in the range 3% to 10%, and smoldering around 15% to 20%. These observations may be tied to the argument (Andreae et al., 1988) that airborne sampling is biased toward flaming combustion (and ground sampling toward smoldering) because vigorous, flaming combustion produces hotter, more buoyant plumes which rise in the atmosphere more than those from smoldering. In any case, our $CO:CO_2$ ratios are consistent with other ground-based measurements, although at the high end of the range, 14% to 19%, even under conditions of apparent flaming combustion. CH_4 measurements from other studies span the range 2 to 17 mmol/mol relative to CO_2, and also tend to cluster into lower values from airborne sampling and higher values from the ground. Again our own measurements, 11 to 16 mmol/mol, are at the higher end of (but well within) the range.

Our measurements of the emission ratio for formaldehyde show it to be a ubiquitous product of biomass burning, with a fairly constant emission ratio of about 2.3 mmol/mol relative to CO_2. Although aldehydes, ketones, organic acids, and other oxygenated hydrocarbons are known to be produced in combustion in general, we are not aware of other similar measurements of CH_2O for comparison. Formaldehyde, as a source of HO_2 radicals in the atmosphere (Warneck, 1988; Finlayson-Pitts and Pitts, 1986), will play an important role in photochemistry and ozone production in aging plumes from biomass fires.

The results for ammonia and nitrous oxide are perhaps of most interest. In all fires, NH_3 appears to be the major nitrogen-containing gas emitted, about five times greater than NO_x emissions. We measure an $NH_3:CO_2$ ratio of about 8 mmol/mol from sagebrush fires and 1 to 3 mmol/mol from forest slash. Hegg et al. (1988, 1990) report values for $NH_3:CO_2$ of 0.14 to 3.2 mmol/mol from a range of fires, LeBel et al. (1988) measured 0.4 to 2.2 mmol/mol from a Florida wetlands fire, and Andreae et al. (1988) infer 1 to 2 mmol/mol from aircraft measurements of NH_4^+ aerosol in the dry season over Amazonia. Our results thus appear to show significantly greater emissions of NH_3 than previous studies. The remote sensing technique is, however, very suitable for ammonia measurements, because the absorption bands are strong, isolated, unambiguous, and easy to measure (see Figure 30.3) There is also no uncertainty in NH_3 measurements due to collection efficiency or losses during sampling and measurement. Ammonia is a notoriously difficult compound to sample and measure. A significant partitioning of fuel nitrogen into NH_3 instead of NO, NO_2, or N_2O following burning will have important ramifications for the cycling of nutrient nitrogen, because the NH_3 has a very different atmospheric chemistry than the oxygenated species. The NH_3 measurements will be treated in more detail in a forthcoming publication.

The spectra also indicate an upper limit for N_2O emission ratios of 8×10^{-5} relative to CO_2. This value is significantly lower than earlier measurements by other groups (Crutzen et al., 1979, 1985; Cofer et al., 1989, 1990; Hegg et al., 1990), but more in agreement with recent values (Elkins et al., 1990; Lobert, 1989). The discovery of artifact N_2O formation in canister samples from fossil fuel burning plumes (Muzio and Kramlich, 1988; Muzio et al., 1989) has lead to careful revision of measurements and techniques for N_2O from combustion sources, and it is recognized that this artifact may also occur in biomass burning samples. Recent measurements of $N_2O:CO_2$ emissions are of the order of $1–2 \times 10^{-5}$ and lower (Elkins et al., 1990; Lobert, 1989). A soil contribution to N_2O emission is also possible, and may help explain higher observed values (Cofer et al., 1990). We believe our upper limit of 8×10^{-5} for the $N_2O:CO_2$ emission ratio to be significant in that it is the only measurement made which is not subject to any doubt concerning sampling artifacts.

The emissions of all nitrogen species from the four field fires studied (Figure 30.8b) can be compared to the nitrogen contents of the fuels burned. Both sagebrush fires show total emissions of $N:CO_2$ of close to 1%, made up principally of NH_3, NO, and NO_2, with traces of HCN and negligible N_2O. Taking a CO_2:total C ratio of about 0.85, this corresponds to an overall N:C mole ratio of about 0.85% for all measured species. We have measured the elemental compositions of samples of grass, sagebrush, and litter from the F2 site: the samples were divided into separate "fractions" (leaves, twigs, wood, etc.), and the weighted mean compositions determined; the N:C ratios in mole percent were as follows:

Grass and twigs	1.2%
Sagebrush	1.0%
Litter	2.4%

Depending on the fractions of grass, sagebrush, and litter burned, the mean N:C ratio in all burned biomass thus probably lies around 1.3% to 1.5%, which can be compared to the observed ratio of about 0.85%. We can thus account for about 60% of the total fuel nitrogen with the sum of measured NH_3, NO, NO_2, N_2O, and HCN. Lobert et al. (1990) have found from laboratory biomass burning studies that the nitrogen budget cannot be balanced; in general, less than 60% of the total fuel nitrogen can be accounted for in the known nitrogen-containing emissions, ash, etc. They postulate N_2 to be the missing species by default; our results for the sagebrush fires, despite the increased amount of NH_3 observed, would support this conclusion. N_2 cannot be detected in the IR and in the presence of atmospheric N_2, and we have not yet seen any spectral features which might be attributable to other major nitrogen-bearing species.

For the two forest waste fires we have not measured fuel nitrogen contents, but they are expected to be much lower than those for sagebrush, of the order of 0.2% to 0.4% for wood and somewhat higher for bark, twigs, and litter. The total N:C emissions of about 0.1% for the slash pile fires (F3) and about 0.3% for the broadcast burn (F5) are in qualitative agreement with these estimates, but again the measured N:C ratios in emissions are lower than fuel N:C ratios. In the case of the slash piles, which consisted mainly of stemwood and large branches, there was very little small fuel, needles, or litter. In contrast, the ground layer of litter and the top layer of soil burn with the broadcast fire, with consequent higher emissions of nitrogen detected.

The simultaneous measurements of several species provided by FTIR long-path absorption spectroscopy also provide valuable insight into the relationships between biomass burning emissions and fire parameters. Our laboratory studies (Figure 30.9), and those of others (e.g., Lobert, 1989; Lobert et al., 1990), consistently show that flaming combustion produces more highly oxidized products such as CO_2 and NO, while smoldering leads to increased emissions of more reduced species such as CO, CH_4, and NH_3. Measurements of emission ratios for flaming versus smoldering combustion, and estimation of the proportion of flaming versus smoldering combustion in any one fire or fire type, are two of the most important quantities required for good estimates of local, regional, and global emissions of trace gases from biomass burning.

Figures 30.4 and 30.5, combined with visual observations as outlined above, demonstrate semi-quantitatively the variation of emission ratios with flaming and smoldering combustion. At time B the decrease of both CO and CH_4 emission ratios with the onset of flaming combustion can be clearly seen. For CH_4 it is particularly marked, with a decrease of a factor of two from 16 to 8 mmol/mol, while for CO the decrease is less marked, from 16% to 13%. The CO values are at the high end of the range compared to other measurements, and are discussed below together with results from other fires. In Figure 30.7, NH_3 appears to increase at the start of flaming combustion, but the precision in this case is lower and this observation may or may not be significant.

The results from the laboratory studies provide more insight into flaming-smoldering differences, since in the laboratory fires these two combustion phases are well separated in time. Figure 30.9 clearly shows the increase in CO and CH_4, and the shift from NO/NO_2 to NH_3 emission, in the smoldering phase compared to flaming. While NO and NO_2 are the dominant detectable nitrogen species during flaming combustion, in two cases they fall below the detection limits during smoldering and NH_3 is dominant. There is also a suggestion in the data that the total detected nitrogen emission is lower during flaming; this may be related to possible N_2 emission but may also be an artifact of the measurement precision. A more complete analysis of all spectra of the laboratory fires will shed more light on these issues. The analysis of these spectra is considerably more time consuming because of the variation in stack temperature from 30°C to 150°C during a fire and will be carried out in full using the spectral fitting techniques outlined in the previous section.

Acknowledgments

We have pleasure in thanking many people for their willing help and cooperation in making this project possible in a tight schedule: Jack Fox and the NCAR machine shop for construction and mounting of the optical components with the FTIR spectrometer; the operational fire staff of the Bureau of Land Management, Casper, Wyoming, and U.S. Forest Service, Superior and Missoula, Montana, for lighting the fires and stopping the trailer from burning down; and staff of the Intermountain Fire Sciences Laboratory (Ron Babbit, Lyn Weger, Pat Boyd, Ron Susott) for support in all Missoula measurements. David W. T. Griffith is grateful for a senior Fulbright fellowship and to the National Center for Atmospheric Research for financially supporting the study. The National Center for Atmospheric Research is sponsored by the National Science Foundation.

REFERENCES

Andreae, M. O., E. V. Browell, M. Garstang, G. L. Gregory, R. C. Harriss, G. F. Hill, D. J. Jacob, M. C. Pereira, G. W. Sachse, A. W . Setzer, P. L. Silva Dias, R. W. Talbot, A. L. Torres, and S. C. Wofsy, 1988: Biomass burning emissions and associated haze layers over Amazonia. *J. Geophys. Res., 93,* 1509-1527.

Cofer, W. R., J. S. Levine, P. J. Riggin, D. I. Sebacher, E. L. Winstead, E. F. Shaw, J. A. Brass, and V. G. Ambrosia, 1988: Trace gas emissions from a mid-latitude prescribed chaparral fire. *J. Geophys. Res., 93,* 1653-1658.

Cofer, W. R., J. S. Levine, D. I. Sebacher, E. L. Winstead, P. J. Riggan, B. J. Stocks, J. A. Brass, V. G. Ambrosis and P. J. Boston, 1989: Trace gas emissions from chaparral and boreal forest fires. *J. Geophys. Res., 94,* 2255-2259.

Cofer, W. R., J. S. Levine, E. L. Winstead, P. J. LeBel, A. M. Koller, and C.R. Hinkle, 1990: Trace gas emissions from burning Florida wetlands. *J. Geophys. Res., 95,* 1865-1870.

Crutzen, P.J., and M. O. Andreae, 1990: Biomass burning in the tropics: Impact on atmospheric chemistry and biogeochemical cycles. *Science, 250,* 1669-1678.

Crutzen, P. J., L. E. Heidt, J. P. Krasnec, W. H. Pollock, and W. Seiler, 1979: Biomass burning as a source of atmospheric gases CO, H_2, N_2O, NO, CH_3Cl, and COS. *Nature, 282,* 253-256.

Crutzen, P. J., A. C. Delany, J. Greenberg, P. Haagenson, L. E. Heidt, R. Lueb, W. H. Pollock, W. Seiler, A. Wartburg, and P. Zimmerman, 1985: Tropospheric Chemical Composition Measurements in Brazil During the Dry Season. *J. Atmos. Chem., 2,* 233-256.

Delany, A. C., P. Haagensen, S. Walters, A. F. Wartburg, and P. J. Crutzen, 1985: Photochemically Produced Ozone in the Emission From Large Scale Tropical Vegetation Fires. *J. Geophys. Res., 90,* 2425-2429.

Elkins, J. W., B. D. Hall, and J. H. Butler, March 1990: *Laboratory and field investigations of the emissions of nitrous oxide from biomass burning.* Paper presented at the Chapman Conference on Global Biomass Burning: Atmospheric, Climatic, and Biospheric Implications, Williamsburg, VA, 19-23 March.

Finlayson-Pitts, B. J., and J. N. Pitts Jr., 1986: *Atmospheric Chemistry: Fundamentals and Experimental Techniques*. New York: John Wiley.

Greenberg, J. P., P. R. Zimmerman, L. E. Heidt, and W. Pollock, 1984: Hydrocarbon and Carbon Monoxide Emissions from Biomass Burning in Brazil. *J. Geophys. Res., 89,* 1350-1354.

Haaland, D. M., and R. G. Easterling, 1980: Improved Sensitivity of Infrared Spectroscopy by the Application of Least Squares Methods. *Appl. Spectrosc.,* 34, 539-548.

Hegg, D. A., L. F. Radke, and P. V. Hobbs, 1988: Ammonia emissions from biomass burning. *Geophys. Res. Letts., 15,* 335-337.

Hegg, D. A., L. F. Radke, and P. V. Hobbs, 1990: Emissions of some trace gases from biomass fires. *J. Geophys. Res., 95,* 5669-5675.